

# INVESTIGATING THE CREEP BEHAVIOR OF MARINE SOFT STRUCTURED CLAY BY FEM WITH AN ELASTO-VISCOPLASTIC CONSTITUTIVE MODEL

M.J. Jiang<sup>\*\*\*</sup>, C.O. Woyeya<sup>1</sup>, J. Liu<sup>1</sup>

<sup>1</sup> Department of Civil Engineering, Tianjin University, 135 Yaguan Road,  
Tianjin 300350, China

\* Corresponding author: [mingjing.jiang@tju.edu.cn](mailto:mingjing.jiang@tju.edu.cn)

**Keywords:** Elasto-viscoplastic Constitutive model, Creep behavior, Marine soft-structured clay, Drained condition, Undrained condition.

**Abstract.** The time-dependent creep deformation of marine soft-structured clay is a major cause of foundation failure on soft grounds around the globe. This study focuses on the analysis of the drained and undrained time-dependent creep behavior of a normally consolidated (NC)-Kyuhoji marine soft-structured clay by FEM with a new Elasto-viscoplastic (EVP) constitutive model. One-dimensional creep and consolidated undrained creep element tests are simulated to analyze the creep behavior of soft clay under constant load conditions. The creep period of 1157days is used in the drained state with consolidation pressures from 100 kPa to 450 kPa with 50 kPa incremental intervals. The undrained time-dependent creep behavior of Kyuhoji clay is analyzed under varying constant creep stresses- $q_{crp}$  ( $0.3q_f$ ,  $0.5q_f$ ,  $0.6q_f$ , and  $0.7q_f$ , where  $q_f$  is the undrained peak strength), and creep periods (11.6days, 463 days, and 5787days). The results show the capability of the new EVP model in analyzing creep failure behavior of marine soft-structured clayey and can explain the reason for the premature abrupt collapse of foundations on soil grounds where drainage is impeded under constant load.

## 1. INTRODUCTION.

The study of rheological creep behaviors of soft cohesive soils by many geotechnical scholars has been ongoing around the globe for over seven decades now. The fueling force behind this is the increase in demand for land as a result of the increasing global population, urbanization, and industrialization around seashores which has triggered land reclamation. As such, more research is required to understand the complex coupled mechanical behavior of remolded and soft-structured marine clay using experimental models, advanced analytical models, and numerical methods like; Finite Element Method (FEM), Discrete Element Method (DEM), and the finite difference method (FDM). For the case of FEM, the initial classical models developed in the 19<sup>th</sup> century like the Modified Cam clay (MCC) [1] and Mohr-Coulomb models for remolded soils idealize soil as a perfect elastic-plastic material and ignores the effect of viscous nature of these soils under full saturation. Hence many scholars have labored to improve these classical models into Elasto-viscoplastic models [2, 3, 4] capable of capturing the effects of initial soil structural and viscous nature on the short and long-term mechanical behavior of soft soils.

An experimental study using indoor consolidated undrained triaxial creep tests on Qingyi River clay was conducted [5] using separate loading methods under varying confining pressures and deviator stresses to establish a new constitutive model. The new model indicated that rheological creep strain is divided into instantaneous deformation stage, attenuation creep stage and steady creep stage under undrained state. The rate of creep strain was dependent on creep load which was a percentage of the soil's peak strength.

In the study of creep in geomaterials particularly on soft clay [6, 7] advanced soft clay creep models which can effectively account for the anisotropy, initial soil structure, and rate dependence of soft soil was used to analyze the settlement performance of test embankments on Murro clay and Boston Blue clay. Using one set of material properties obtained from the indoor and field tests, the results from the analyses coincided well with the field-measured settlements. Hence advanced soft soil creep models are currently vital tools for use by geotechnical engineers in understanding complex coupled soil-water mechanical behaviors of soft grounds under loading.

In this paper, the drained and undrained time-dependent creep behavior of normally consolidated (NC)-Kyuhoji marine soft-structured clay is analyzed by finite element (FEM) ABAQUS software with an advanced combined super-loading and sub-loading yield surface Elasto-viscoplastic (EVP) constitutive model. One-dimensional creep and consolidated undrained triaxial creep element tests are simulated to analyze the creep behavior of soft-structured marine clay under constant stress conditions. The effect of pre-consolidation pressure in drained creep settlement, the creep stress level and creep periods on undrained creep behavior and undrained shear strength are analyzed and discussed

## 2. ELASTO-VISCOPLASTIC CONSTITUTIVE MODEL AND FEM SIMULATION PROCEDURES.

### 2.1. The new Super-Subloading Elasto-viscoplastic model

This model was developed from modification of Elasto-plastic models like MCC-model for NC-remolded clay, Subloading and Superloading yield surface models for overconsolidated and structured clay respectively [8], [9]. The new advanced model was proven effective in predicting the time-dependent behavior of NC, overconsolidated and structured clay after calibration to incorporate material properties of Kyuhoji marine clay [10].

In Fig.1(a),  $(p', q)$  is the current dynamic stress state;  $(p'_w, q_w)$ ,  $(p'^*_w, q'^*_w)$  and  $(\bar{p}'_w, \bar{q}'_w)$  the corresponding mean effective stress and the deviator stress on the sub-loading, original Can clay, and super-loading yield surfaces for overconsolidated, NC, and soft-structured clay respectively. It was assumed that these parameters obey the following relation;  $\frac{q_w}{p'_w} = \frac{q'^*_w}{p'^*_w} = \frac{\bar{q}'_w}{\bar{p}'_w}$  and the similarity ratios of their intercepts in the mean effective stress  $p'$  axis is given by;  $\frac{\bar{p}'_m^{(w)}}{p'_m^{(w)}} = \frac{1}{R}$  which defines the over consolidation ratio (OCR) denoted by  $\omega$ , where  $\omega \geq 1$  and  $\frac{\bar{p}'_m^{(w)}}{p'^*_m^{(w)}} = \frac{1}{R^*}$  defines the initial soil structure parameter denoted by  $\zeta$ , where  $0 < \zeta \leq 1$  with  $\zeta = 1$  means the soil is at full destructuration.

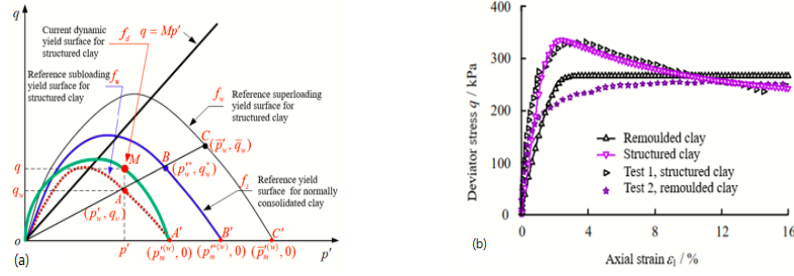


Figure 1: (a) Relationship between yield surfaces, (b) stress-strain relationship of Kyuhoji marine clay.

The validation of the EVP model was done by comparing the numerical simulation results of a consolidated undrained triaxial test with soil mechanical parameter of Kyuhoji soft-structured clay in Table 1 below, with the experimental results (Fig.1 (b)) [11]. The numerical results for structured clay match well with the experimental results hence confirming the efficacy of the EVP model in predicting the mechanical behavior of structured clay under load.

**Table 1:** Model material properties.

Parameters symbols	$\nu$	$e_0$	$M=q/p'_m$	$\lambda$	$\kappa$	$c_0$	$m'$	$A$	$\beta$	$\zeta$	$\omega$	$\Theta$	$C$
SI-Units						$s^{-1}$							kPa
Values	0.39	1.41	1.49	0.327	0.028	6.27e-11	21.5	0.5	5	0.55	1.15	0.5	10

Where:  $\nu$ -Poisson's ratio,  $e_0$ -Initial void ratio when  $p'_m=1\text{kPa}$ ,  $M=q/p'_m$ -Stress ratio at a critical state,  $\lambda$ -Compression index,  $\kappa$ -Swelling index,  $c_0$ -Coefficient of viscosity,  $m'$ -Overstress parameter,  $\alpha$ -Dissipation coefficient of OCR,  $\beta$ -Dissipation coefficient of soil structure,  $\zeta$ -Initial structural parameter,  $\omega$ -Over consolidation ratio,  $\Theta$ -Time integrating factor, and  $C$ -the internal forces of the cohesive.

## 2.2. Simulation procedures for Element test.

In this study, the mechanical parameters as shown in Table-1 with  $\zeta=0.55$  to represent marine soft-structured clay are used together with the EVP-model stress algorithm incorporated in FEM-Abaqus software to simulate the drained and undrained creep behavior of marine clay at element test level. Calibration of experimental data for the EVP-model can be found in [12].

### 2.2.1. One-dimensional creep test.

A one-dimensional creep test using a separate loading method was simulated using the mechanical parameters for Kyuhoji soft-structured marine clay to study its drained creep behavior at constant effective stress. An Axisymmetric model to depict half of a cylindrical standard size for a one-dimensional consolidation test specimen in the laboratory was modeled. The bottom boundaries are fully fixed and the right vertical side boundary was fixed laterally and allowed to move in the vertical direction, while axisymmetric conditions set on the left vertical boundary as illustrated in Fig.2(a) The top and bottom surfaces are allowed to drain while vertical consolidation stress- $\sigma_v$  from 100 kPa to 450 kPa in 50 kPa incremental ranges is

applied separately from the top boundary as shown in Fig.1(b). For each stress, excess pore water pressure is allowed to dissipate fully, then, creep settlement is monitored at constant effective stress.

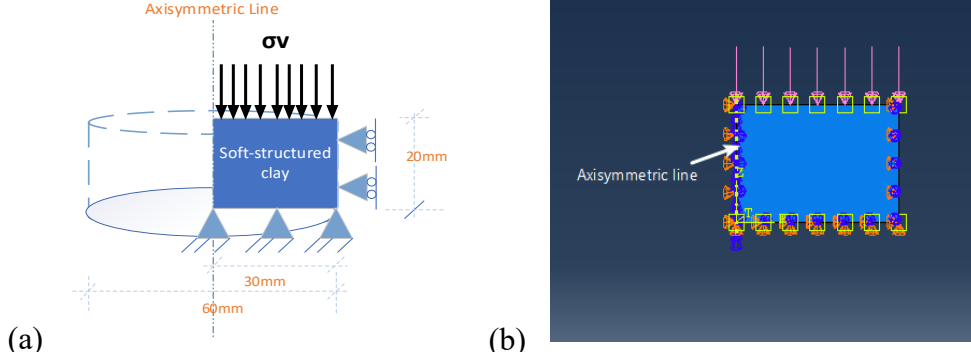


Figure 2: (a) the schematic model of the standard cylindrical size of 60mm height and 20mm diameter for analysis, (b) the axisymmetric model in Abaqus for one-dimensional creep test analysis.

A creep period of 1157 days is allowed while maintaining the same consolidation stress on the soil model and monitoring the creep behavior.

### 2.2.2. Consolidated undrained triaxial creep test.

To simulated the undrained triaxial creep test, a conventional consolidated undrained triaxial creep tests for different confining pressures- $\sigma_3$  (200 kPa, 250 kPa, 300 kPa, and 350 kPa) was simulated at 0.1% strain rate with 10% axial strain, and the respective undrained peak strength- $q_f$  obtained as shown in Table 2. Similarly, axisymmetric conditions are assumed to depict half of the standard cylindrical model of height 80mm by 20mm width as shown in Fig.3(a) and considered for analysis. Hence an axisymmetric model as seen in Fig.3(b) is simulated in FEM-Abaqus to mimic separate loading triaxial creep test procedure in the laboratory.

Table 2: Undrained peak strength and the creep loads for analysis

Cell pressure- $\sigma_3$ (kPa)	Peak strength- $q_f$ (kPa)	$0.3q_f$ (kPa)	$0.5q_f$ (kPa)	$0.6q_f$ (kPa)	$0.7q_f$ (kPa)
200	186	55.8	93	111.6	130.2
250	235	70.5	117.5	141	164.5
300	282	84.6	141	169.2	197.4
350	330	99	165	198	231

A series of consolidated undrained triaxial creep tests were simulated for stress levels- $q_{crp}$  of  $(0.3q_f, 0.5q_f, 0.6q_f, \text{ and } 0.7q_f)$  for the specified cell pressures with varying creep periods of 11.6days, 463days and 5787 days. The creep behavior of the NC marine soft-structured clay is

studied by monitoring the behavior of stress path, excess pore pressure, and axial strain in undrained conditions at constant creep stress. After the specified creep period, the specimen was sheared by time-controlled vertical displacement, and the effect of creep on undrained shear strength of NC marine soft-structured clay was analyzed.

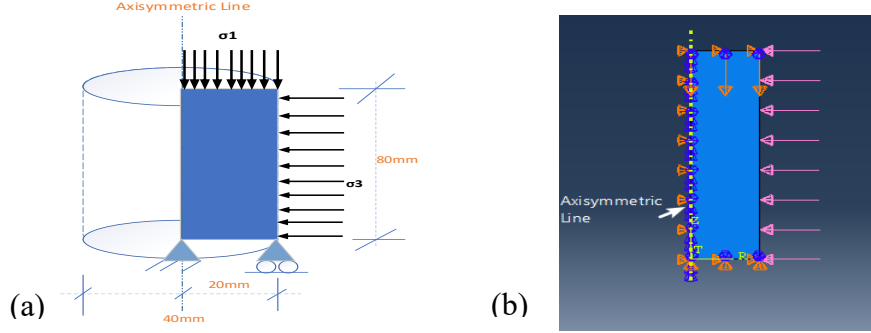


Figure 3: (a) the schematic model of the standard cylindrical size of 80mm height and 40mm diameter for analysis, (b) the axisymmetric model in Abaqus for consolidated undrained triaxial creep test analysis.

### 3. RESULT ANALYSIS AND DISCUSSION

#### 3.1. Effect of pre-consolidation pressure on the drained creep behavior of marine soft-structured clay (1D creep analysis).

The creep secondary compression settlement occurs at constant effective stress. For marine soft-structured clay, it was highly predicted to be as a result of destructuration by interparticle bond breakage and fabric repacking hence reduction in soil's specific volume [13]. As such, secondary compression settlement due to creep was observed to decrease with an increase in consolidation pressure (Fig. 4(a)). For  $\sigma_v$  of 100 kPa, creep settlement of 2.2mm was recorded which is about 11% of the soil layer thickness, 1.85mm (9.3%) for 150 kPa, 1.3mm (6.5%) for 200 kPa, and an average value of about 1.15mm (5.8%) for consolidation pressure from 250 kPa to 450 kPa without significant change.

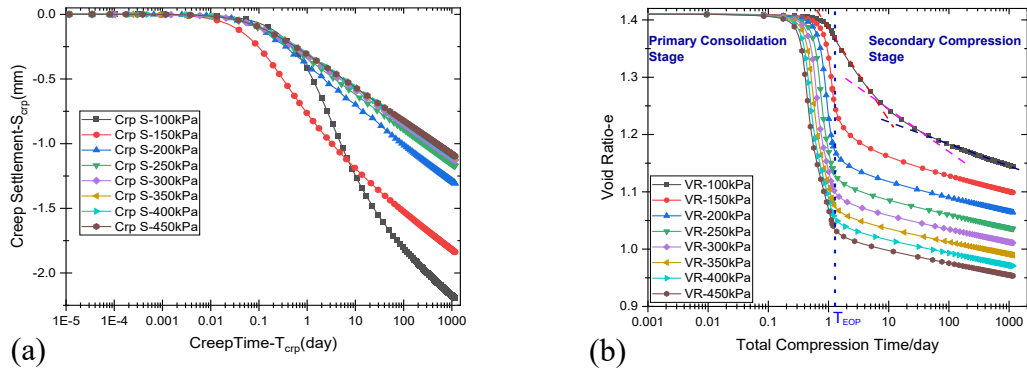


Figure 4: The relation of (a) Creep secondary compression settlement (b) void ratio versus compression  $\log t$

From the relationship of void ratio- $e$  with time on the log scale ( Fig. 4(b)), after the end of primary consolidation period- $T_{EOP}$  of one day, it is observed from the S-shaped curves of the  $e$ - $\log t$ , that the secondary compression index- $C_\alpha$  decreases from  $\sigma_v = 100$  kPa to 300 kPa and the

becomes almost constant for values of  $\sigma_v$  from 300 kPa to 450 kPa attaining the isotach behavior. From the experimental results [10] on Kyuhoji marine soft-structured clay, its pre-consolidation pressure- $\sigma_c$  was about 330 kPa. This means that the  $C_a$  value for this soft-structured clay decreases from  $\sigma_v = 100$  kPa to  $\sigma_c$  value and becomes constant for values of  $\sigma_v \geq \sigma_c$ . This means that  $C_a$  for this homogeneous marine soft-structured is dependent on the pre-consolidation pressure.

### 3.2. Effect of creep on the stress-Path during the undrained creep state at constant stress.

From Fig.5 (a)-(d), it was observed that after application of creep stress- $q_{crp}$ , the soil current stress state line (CSSL) tends to move towards the critical state line (CSL) as mean effective stress decreases at constant deviatoric stress. The  $0.7q_f$  case is seen to have reached CSL in 11.6 days creep period, while  $0.6q_f$ ,  $0.5q_f$ , and  $0.3q_f$  still in a stable stress state. This implicitly indicates that soil is experiencing time-dependent shear strain hence transiting to failure. However, the rate of transition from the CSSL to CSL depends on both creep time and the magnitude of  $q_{crp}$ .

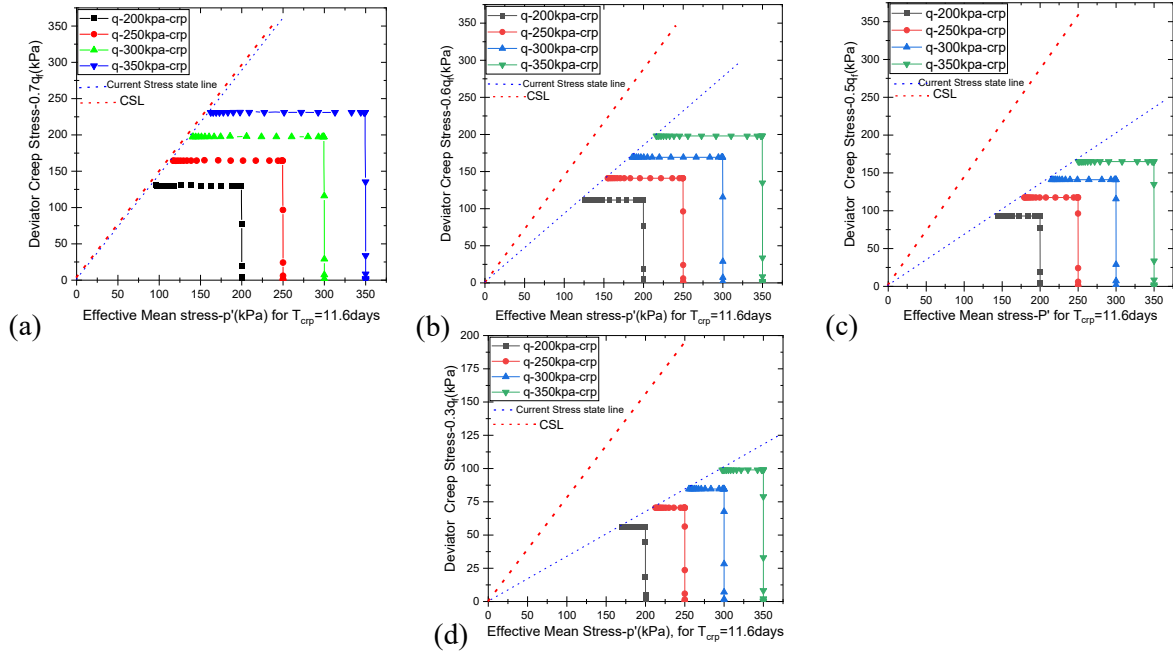


Figure 5: Stress paths for (a)  $0.7q_f$ , (b)  $0.6q_f$ , (c)  $0.5q_f$ , and (d)  $0.3q_f$  for 11.6 days creep period in undrained conditions

After the failure of the  $0.7q_f$  case, the  $0.6q_f$ ,  $0.5q_f$  and  $0.3q_f$  creep load cases were monitored for a creep period of 463 days. Fig.6 (a)-(c) shows that after this period, the soft-structured clay at  $0.6q_f$  has reached the CSL, while the  $0.5q_f$  case CSSL is about to match the CSL implying at the verge of failure. However, the  $0.3q_f$  case CSSL was still far away from the CSL.

Creep analysis for 5787 days of creep period in the undrained state was done for  $0.5q_f$  and  $0.3q_f$ , and as seen from Fig.7 (a), the results show that the  $0.5q_f$  case CSSL almost matches with

the CSL implying that soil has failed. However, the stress path for  $0.3q_f$  (Fig.7(b)) shows that the stress state is not yet at the CSL, hence still apparently stable.

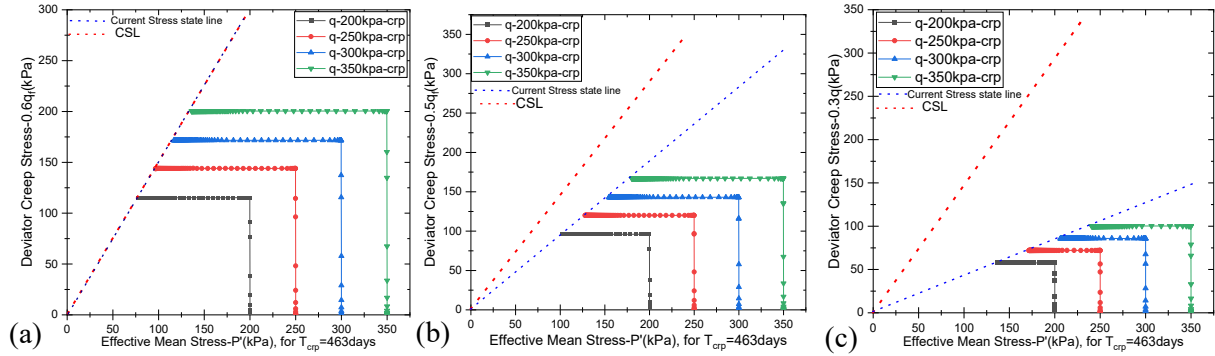


Figure 6: Stress paths for (a)  $0.6q_f$ , (b)  $0.5q_f$ , and (c)  $0.3q_f$  for 463 days creep period in undrained conditions

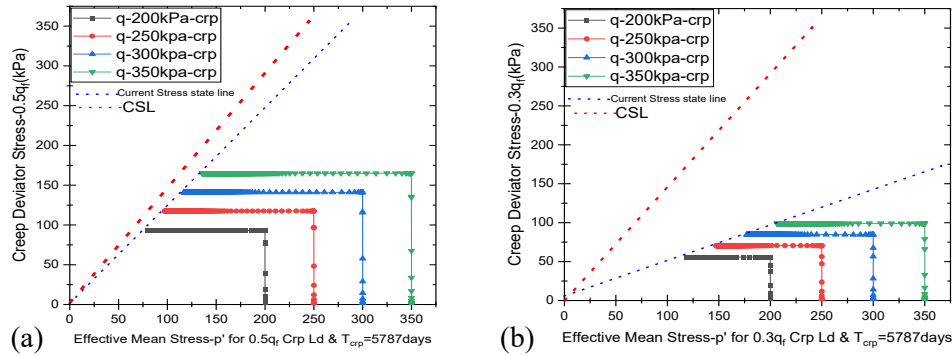


Figure 7: Stress paths for (a)  $0.5q_f$  and (b)  $0.3q_f$  for 5787 days creep period in undrained conditions

### 3.3. Behavior of axial strain of marine soft-structured clay during undrained and constant creep load conditions.

From the analysis of the consolidated undrained triaxial creep test simulation, the axial strain versus creep time in days was output for  $q_{crp}$  from  $0.7q_f$ – $0.3q_f$  for different confining pressure as shown in Fig.8 (a)–(c). It is observed that after the application of creep load, the rate of axial strain was low, then increased to moderate, and finally acceleration stage. The rate of change in axial strain from low to moderate, and acceleration depends on the magnitude of  $q_{crp}$ . From Fig.8(a)–(c), for all cases of creep periods, it is evident that the rate of creep axial strain increased with the magnitude of  $q_{crp}$ , showing  $0.7q_f$  reaching the acceleration stage in 11.6 days before  $0.6q_f$ ,  $0.5q_f$  and  $0.3q_f$  case. However, it can be seen that creep axial strain is higher for lower confining pressures of 200 kPa to 250 kPa as compared to 300 kPa and 350 kPa. After 463 days creep period, the axial strain of  $0.6q_f$  case also reached the acceleration stage (Fig.8(b)) which implies failure, while the  $0.5q_f$  case entered the acceleration stage after 5787 days before the  $0.3q_f$  case (Fig.8(c)). Generally, it is concluded in this study that indeed the rate of axial strain of soft-structured marine clay in undrained state at constant load conditions increases with an increase in creep stress, and creep time, but decreases with an increase in the magnitude of confining pressure.

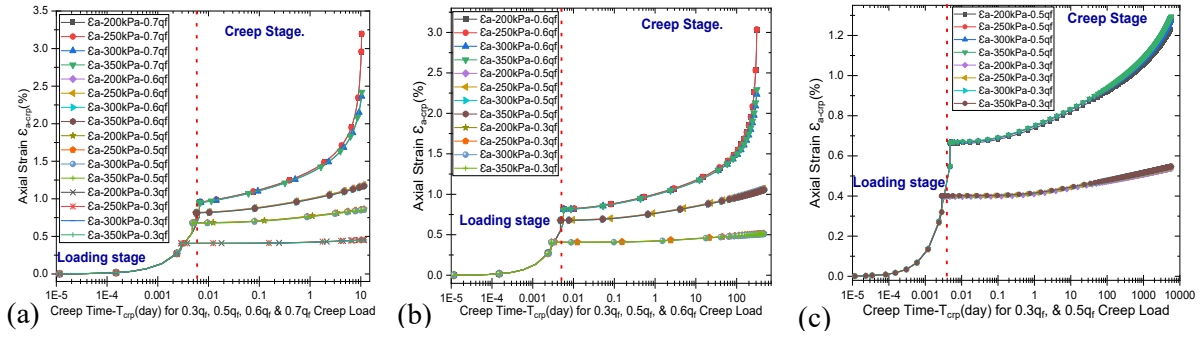


Figure 8: Creep axial strain with  $\log t$  (days) for; (a) 11.6 days, (b) 463 days, and (c) 5787 days

This finding was in agreement with the recent experimental study of the triaxial creep behavior of compacted structured red clay of a roadbed in the southwest of China [14], proving the efficacy of the EVP model in use.

### 3.4. Deviator and Excess Pore water pressure versus axial strain during undrained creep state under constant load.

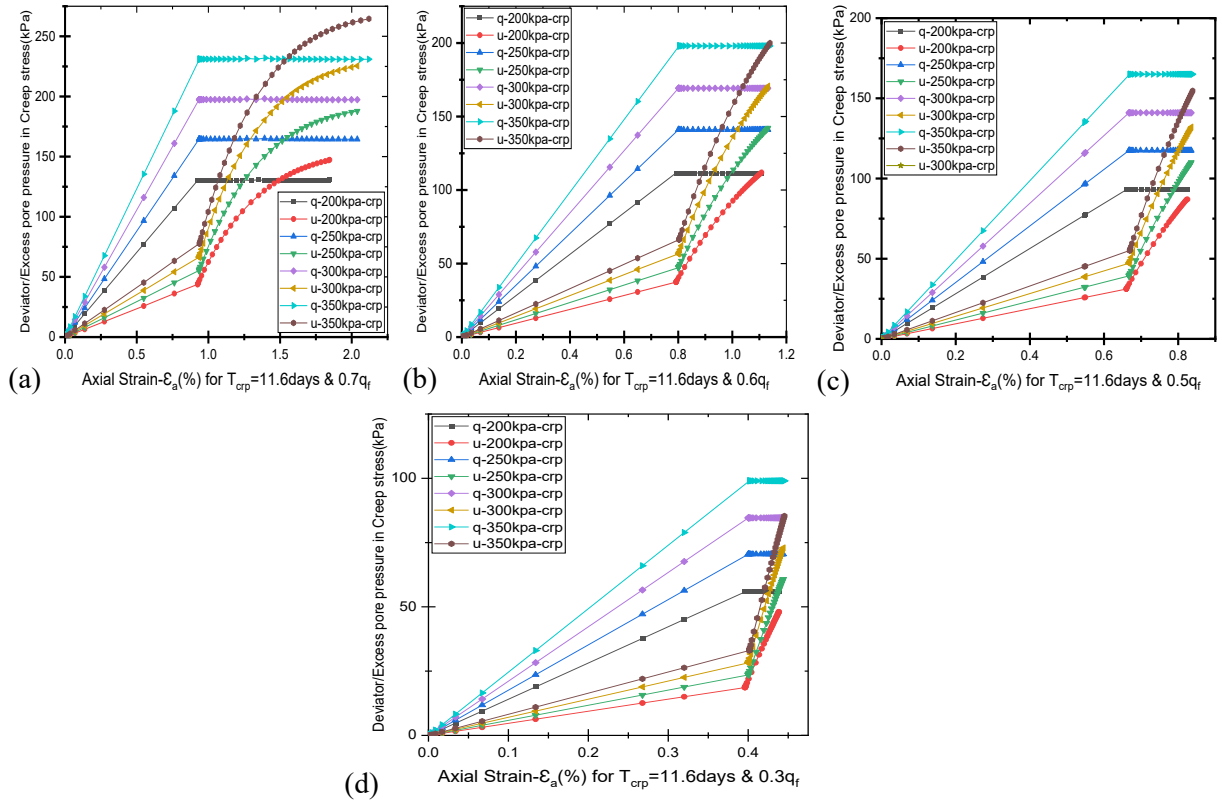


Figure 9: The variation of deviator stress and pore pressure with axial strain for; (a)  $0.7q_f$ , (b)  $0.6q_f$ , (c)  $0.5q_f$ , (d)  $0.3q_f$  for 11.6 days creep period.

To analyze the creep progressive failure of NC soft-structured marine clay in an undrained state at constant load, the excess pore water pressure- $u$  and deviator stress which is  $q_{crp}$  was plotted against the axial strain for creep periods of 11.6 days, 463 days, and 5787 days as shown

in Fig.9, and 10. For the case of 11.6 days creep period as shown in Fig.9 (a)-(d), it was observed that after application of  $q_{crp}$ ,  $u$  increased with axial strain, and time while  $q_{crp}$  was constant. The rate of increase in  $u$  depends on the magnitude of  $q_{crp}$  applied as a percentage of  $q_f$ , hence it is seen that the increase of  $u$  is highest for  $q_{crp}=0.7q_f$ , followed by  $0.6q_f$ , then  $0.5q_f$ , and finally  $0.3q_f$ . It is imperative to note that the after creep load was fully applied and creep deformation allowed to occur, growth in  $u$  was rapid, then gradual, and finally constant as seen in the  $0.7q_f$  case. This can be related to the preceding observations in stress paths and axial strain-log  $t$  analyses and concluded that the growth of  $u$  diminishes as the soil tends to critical state stress and acceleration stage of axial strain which is failure state.

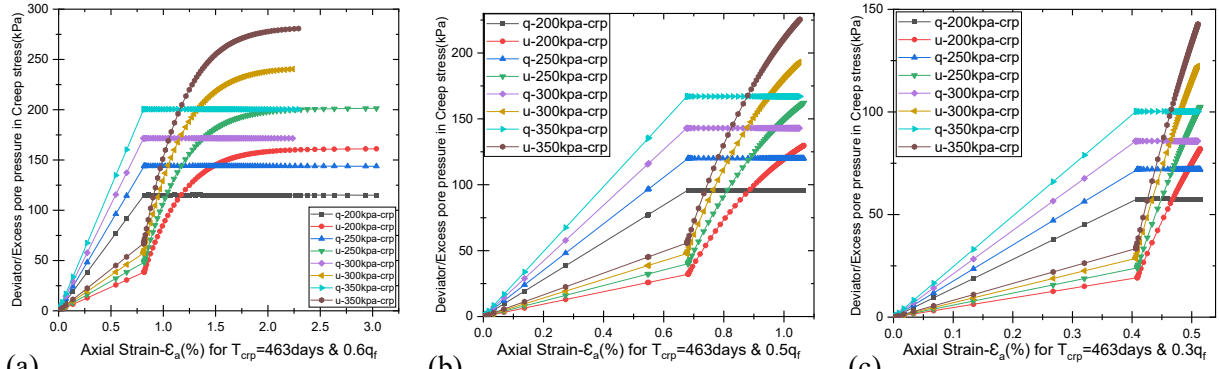


Figure 10: Variation of deviator stress and pore pressure with axial strain for (a)  $0.6q_f$ , (b)  $0.5q_f$ , (c)  $0.3q_f$  for 463 days creep period.

After the growth of  $u$  was constant for  $0.7q_f$  case (failure),  $0.6q_f$ ,  $0.5q_f$ , and  $0.3q_f$  case were monitored for 463 days creep period, and from Fig.10 (a)-(c), it is observed that the growth of  $u$  diminishes attaining a constant value of  $u > q_{crp}$ , which means failure stage when related to the findings in Fig.6. The  $0.5q_f$  and  $0.3q_f$  cases were then analyzed for 5787 days creep period and the same behavior manifested, with the  $0.5q_f$  case on the verge of failure while for the  $0.3q_f$  case, the growth of  $u$  was still in the rapid stage. These findings are similar to what was obtained in [15] studies. In conclusion, the growth of excess pore pressure- $u$  at constant stress is the major cause of foundation failure in soft soils with low hydraulic conductivity. The rate of growth in  $u$  depends on the magnitude of applied stress and also the time of loading when drainage is impeded. This prediction can not be obtained from the analytical methods because they idealize soil as perfect elastic material which is not realistic. Quantitatively, it is seen that the new EVP model can give realistic behavior of pore water pressure increase at constant load in undrained conditions for soft-structured marine clay, hence can be applied in solving real-life challenges in Geotechnics.

### 3.5. Effect of creep on the undrained shear strength of soft-structured marine clay.

The effect of creep on undrained shear strength was analyzed by shearing the soil model to complete failure at the end of creep periods. From Fig. 12 (a)-(b) for 11.6 days creep period, the stress path of  $0.7q_f$  case shows softening state, while  $0.6q_f$  case indicating transition into softening, and  $0.5q_f$  case in hardening stage with a peak strength of soil that underwent creep higher than that of soil with no creep, and also  $0.3q_f$  case indicating the beginning of hardening.

The observations indicate that in an undrained state under constant load, marine soft-structured clay soil initially undergoes creep-hardening, then softening to failure. The softening can be attributed to the growth of excess pore pressure at constant load which lows the soil's effective stress. However, the rate of hardening and softening also depends on the magnitude of applied stress and creep time. This can explain the reason why most foundations on soft grounds fail abruptly after showing apparent stability for some time from the end of construction. It is important to note that the analytical calculations used in foundation designs can not explicitly predict this time-dependent creep hardening and softening of soil during the service life of structural foundations. Hence the modern geotechnical engineers must embrace the use of these enhanced EVP-constitutive models to give realistic predictions of the creep behavior of soft-structured soils under loading.

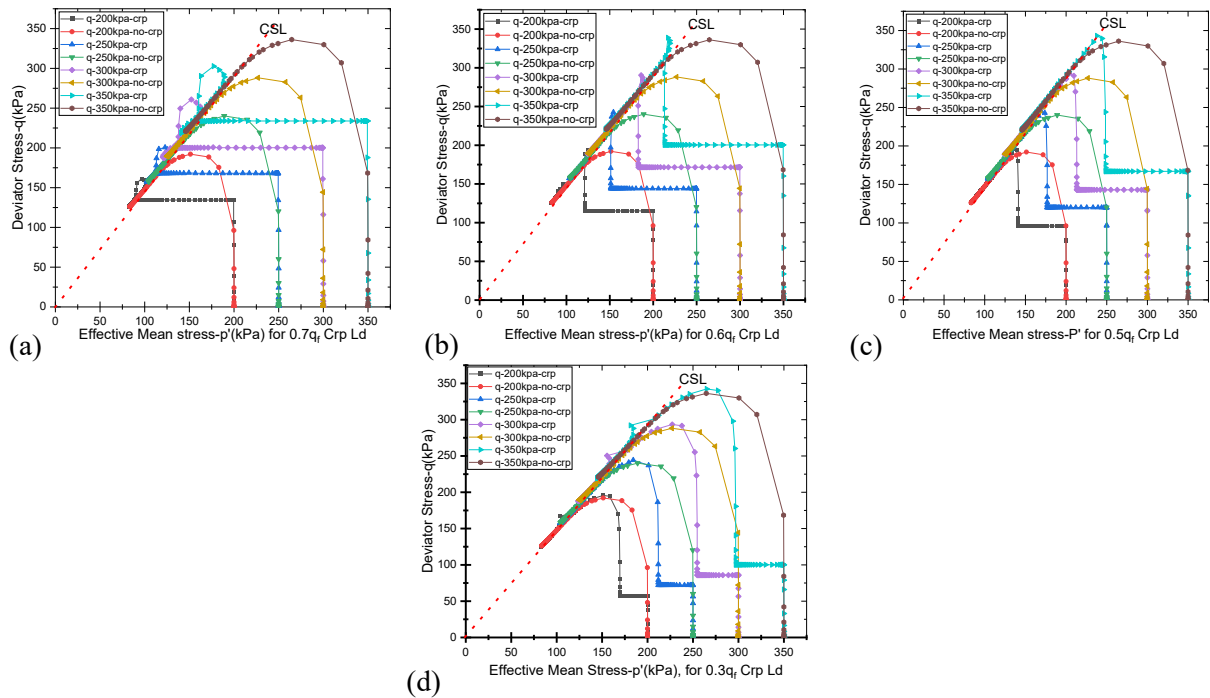


Figure 12: Stress path for 11.6 days creep period for; (a)  $0.7q_f$ ; (b)  $0.6q_f$ ; (c)  $0.5q_f$ ; and (d)  $0.3q_f$  including shearing to failure.

#### 4. CONCLUSION.

The creep behavior of (NC)-Kyuhoji marine soft-structured clay was analyzed in drained and undrained conditions using enhanced super loading-sub loading Elasto-viscoplastic (EVP) constitutive model. One-dimensional creep and consolidated undrained triaxial creep element tests are simulated for creep analysis. The effect of pre-consolidation pressure in drained creep settlement, the creep stress level and creep time on undrained creep behavior, and undrained shear strength was analyzed and discussed

The results show that:

- (1) In the case of the drained state, the secondary compression index,  $C_\alpha$  initially decreases with increasing consolidation pressure from 100 kPa up to pre-consolidation pressure-

$\sigma_c$  and becomes constant for consolidation pressures above  $\sigma_c$ .

- (2) Secondary compression settlement decreases with an increase in the magnitude of the consolidation pressure, which showed the importance of preloading. However, the lowest value of creep settlement was about 5.8% which is still a significant value that requires attention for reduction, especially for structures with high sensitivity to excessive settlement eg. Airports.
- (3) In an undrained state with a constant load, soft-structured marine clay is seen to initially experience creep hardening, then softening due to an increase in excess pore water pressure at constant load up to the failure of soil. This was observed in the stress paths which indicated soil stress state transiting from a stable stress state towards the critical stress state, hence failure.
- (4) The growth in axial strain in an undrained state is initially low, then moderate, and finally rapid indicating the failure zone. The rate of increase in axial strain is both stress and time-dependent.
- (5) The rate of excess pore water pressure growth in undrained conditions under constant load is highly dependent on the magnitude of creep stress- $q_{crp}$  and time.

These results have shown the capability of the new EVP model in analyzing creep failure behavior of marine soft-structured clayey and can explain the reason for the premature abrupt collapse of foundations on soft-structured clay soils where drainage is impeded under constant load.

### Acknowledgments.

The authors are grateful for the research funding from the National Nature Science Foundation of China with Grant Nos. 51890911 and 51639008.

### 5. REFERENCES

- [1] Amorosi, A., and Kavvadas, M.J. A plasticity-based constitutive model for natural soils. a hierarchical approach, in Constitutive Modelling of Granular Materials, D. Kolymbas, Ed. Berlin, Heidelberg: *Springer Berlin Heidelberg* (2000):413–438.
- [2] Islam, M.N., and Gnanendran, C.T. Elastic-Viscoplastic Model for Clays: Development, Validation, and Application. *J. Eng. Mech.*(2017)**143**.
- [3] Mirjalili, M., Kimoto, S., Oka, F and Higo, Y. Elasto-viscoplastic modeling of Osaka soft clay considering destructuration and its effect on the consolidation analysis of an embankment. *Geomechanics and Geoengineering* (2011)**6**:69-86.
- [4] Yin, J.-H., Zhu, J.-G., and Graham, J. A new elastic viscoplastic model for time-dependent behaviour of normally and overconsolidated clays: theory and verification. *Canadian Geotechnical Journal* (2002)**39**.
- [5] Zhao, X., Wang, Q., Gao, Y., Yang, T., He, L., and Lu, X. Indoor Rheological Test and Creep Model Analysis of Soft Soil in Qingyi River region in Wuhu Anhui. *IOP Conf. Ser.: Earth Environ. Sci.*(2019)**330**.

- [6] Grimstad, G., Minna, K., Hans, P.J., Nallathanmby, S., Magne, M., Cor, Z., Haan, E., and Seyed, A.G. Creep of geomaterials – some finding from the EU project CREEP. *European Journal of Environmental and Civil Engineering* (2017):1-16.
- [7] Fatahi, B., Le, T.M., Le, M.Q., and Khabbaz, H. Soil creep effects on ground lateral deformation and pore water pressure under embankments. *Geomechanics and Geoengineering* (2013)**8**:107-124.
- [8] Wang, W., Jiang, M., Shen, Z., Chen, S, and Cai, J. A new method for establishing elastic-viscoplastic constitutive model of clay. *Geomechanics from Micro to Macro*, K. Soga, K. Kumar, G. Biscontin, and M. Kuo (2014):699-704.
- [9] Asaoka, A., Nakano, M., and Noda, T. SUPER LOADING YIELD SURFACE CONCEPT FOR THE SATURATED STRUCTURED SOILS. *Application of Numerical Methods to Geotechnical Problems* (1998)
- [10] Yashima, A., SHIGEMATSU, H., Oka, F., and NAGAYA, J. Mechanical behavior and micro-structure of Osaka Upper-Most pleistocene marine clay. *Proceedings of the japan Society of Civil Engineers* (1999):217-229.
- [11] Wang, Z., JIANG, M., CHEN, S., and CAI, J. An elasto-viscoplastic constitutive model and its stress integration algorithm based on super-subloading yield surface. *Rock and Soil Mechanics*, (2016)**37**:357-366.
- [12] Jiang, M., Pasha, G., and Lu, G. Finite Element Analysis of Strain Localization in Natural Clay Using Elasto-Viscoplastic Constitutive Model. *Resilient Design and Construction of Geostructures Against Natural Hazards*, (2021):110–119.
- [13] Budhu, M. Soil mechanics and foundations, 3rd ed. New York: Wiley, (2011).
- [14] Long, Z., Cheng, Y., Yang, G., Yang, D., and Xu, Y. Study on Triaxial Creep Test and Constitutive Model of Compacted Red Clay. *Int J Civ Eng*, (2020).
- [15] Crawford, C.B., Fannin, R.J., and Kern, C.B. Embankment failures at Vernon, British Columbia. *Canadian Geotechnical Journal*, (1995)**32**:271–284.